

Exploring optoelectronics potential of monolayer tungsten diselenide

Three groups have recently reported on preliminary experiments with photovoltaic and light-emission effects from pn junctions created using split-gate electrostatic doping. **Mike Cooke** reports.

Researchers are beginning to explore the semiconductor potential of monolayer materials beyond graphene with hopes of developing robust devices that are flexible and transparent for deployment in wearable formats, interactive displays, and efficient solar cells.

An interesting class of materials that has recently come to the fore is that of few-layer group-VIB transition-metal dichalcogenides (TMDs) such as molybdenum disulfide (MoS_2), molybdenum diselenide (MoSe_2), tungsten disulfide (WS_2), and tungsten diselenide (WSe_2).

The crystal structure consists of the metal atoms encapsulated between two layers of sulfur/selenium chalcogenide atoms. The bonding within a monolayer is strong while the bonding between monolayers is weak. Like with graphene/graphite, the monolayers of TMD can be exfoliated.

Electronically, TMDs in bulk form tend to have an indirect-bandgap semiconductor behavior, meaning that photon emission is very difficult. However, monolayers of TMD have a wider direct bandgap that opens up opportunities for creating optoelectronic devices such as solar cells and light-emitting diodes (LEDs). Monolayers have about 95% transparency, suggesting uses as transparent conductive electrodes. The transparency also points to stacking of devices for solar energy harvesting. Other possibilities include optical interconnect, logic and sensor applications.

Monolayer WSe_2 has a photoluminescence direct bandgap of 1.64eV with a full-width at half maximum (FWHM) of 56meV. The quantum yield from multi-layer WSe_2 reduces with thickness, signaling the transition to an indirect bandgap.

Another feature of monolayer TMDs is that electron-hole interactions are much stronger than in conventional semiconductors due to a large carrier effective mass and reduced screening in two dimensions. This leads to large binding energies for both charged and neutral excitons which, as a result, are spectrally sharp, robust and amenable to electrical manipulation.

Three separate research groups have reported promising preliminary results for WSe_2 devices that can

both convert light into current and current into light. The creation of n- and p-type conductivity in these devices was achieved electrostatically with a split gate beneath the WSe_2 monolayer.

Vienna University of Technology [Andreas Pospischil et al, *Nature Nanotechnology*, vol 9 (2014), p257] began its fabrication by forming a split gate of titanium/gold with a 460nm gap on a silicon/silicon dioxide wafer (Figure 1). Gate bonding pads were also formed with titanium/gold. The split gate was covered with silicon nitride, except for the bonding pads.

WSe_2 flakes were exfoliated from bulk material supplied by Nanosurf onto a stack of polymer layers on a sacrificial silicon substrate. Suitable flakes were identified under an optical microscope. The bottom polymer layers were dissolved in water and the top layer was used to transfer the flake to overlap both sides of the gate electrode by about 900nm. The polymer was then dissolved and anode and cathode electrodes formed.

Palladium was used for the anode hole injector since the metal's high-workfunction Fermi level is aligned to the valence band edge of the WSe_2 monolayer. The cathode was titanium with a low workfunction. Nickel might be a suitable alternative that would be less prone to oxidation.

The device was finally vacuum-annealed for several hours at 380K to remove doping adsorbates and water. Although the device was functional in air, the measurements were carried out under high vacuum to ensure better long-term stability.

Experiments with the split gates shorted together gave a device with an on-off current ratio in the range 100–500. The device exhibits ambipolar characteristics with both electron and hole injection, depending on gate potential. The poor performance as a transistor is attributed to the inefficient gate structure.

A pn junction is created by putting a positive potential on one gate and a negative potential on the other. Under these conditions, the device "clearly shows rectifying behavior".

The n-type resistance of the monolayer under positive gate potential was found to be an order of magnitude

smaller than the p-type resistance under negative gate potential.

Under illumination, the device created a photocurrent when the gates were biased in a pn configuration but not in the resistive p- or n-type modes. The researchers comment: "This is a clear indication that the photoresponse does not arise from one of the Schottky contacts, as it relies on the existence of a p-n junction. Moreover, the photocurrent changes sign when the gate polarities are flipped, which cannot be explained by the built-in potential due to asymmetric contact metallization."

With 1400W/m^2 illumination, the solar cell maximum output power was 9pW at a voltage of 0.64V and current of 14pA . The fill factor compared with the product of the short-circuit current and open-circuit voltage was 0.5. The conversion efficiency was estimated to be 0.5%, similar to values obtained for devices based on bulk WSe_2 . "To our knowledge, this constitutes the first demonstration of efficient photovoltaic energy conversion in a 2D atomic crystal," the researchers write.

The solar cell performance suggests there is shunt resistance associated with recombination losses, indicating room for improvements from material quality enhancement. Reverse biasing the pn junction at -1V gives a photodiode responsivity of 16mA/W .

The pn junction also emitted light with estimated electroluminescence efficiency (η_{EL}) of 0.1% (Figure 2). The researchers comment: "Currently, η_{EL} is limited by resistive losses in R_s and by non-radiative recombination in the WSe_2 . It can therefore be increased by reducing the contact resistance or by using a crystalline substrate to reduce the density of disorder-induced recombination centers."

This light emission compares with electroluminescence efficiency of 0.01% in a similar setup with monolayer molybdenum diselenide (MoSe_2). In the case of MoSe_2 , the light is generated by excitons (electron-hole bound states) resulting from impact excitation. "In contrast, our device is operated as a true light-emitting diode with ambipolar carrier injection," the researchers write.

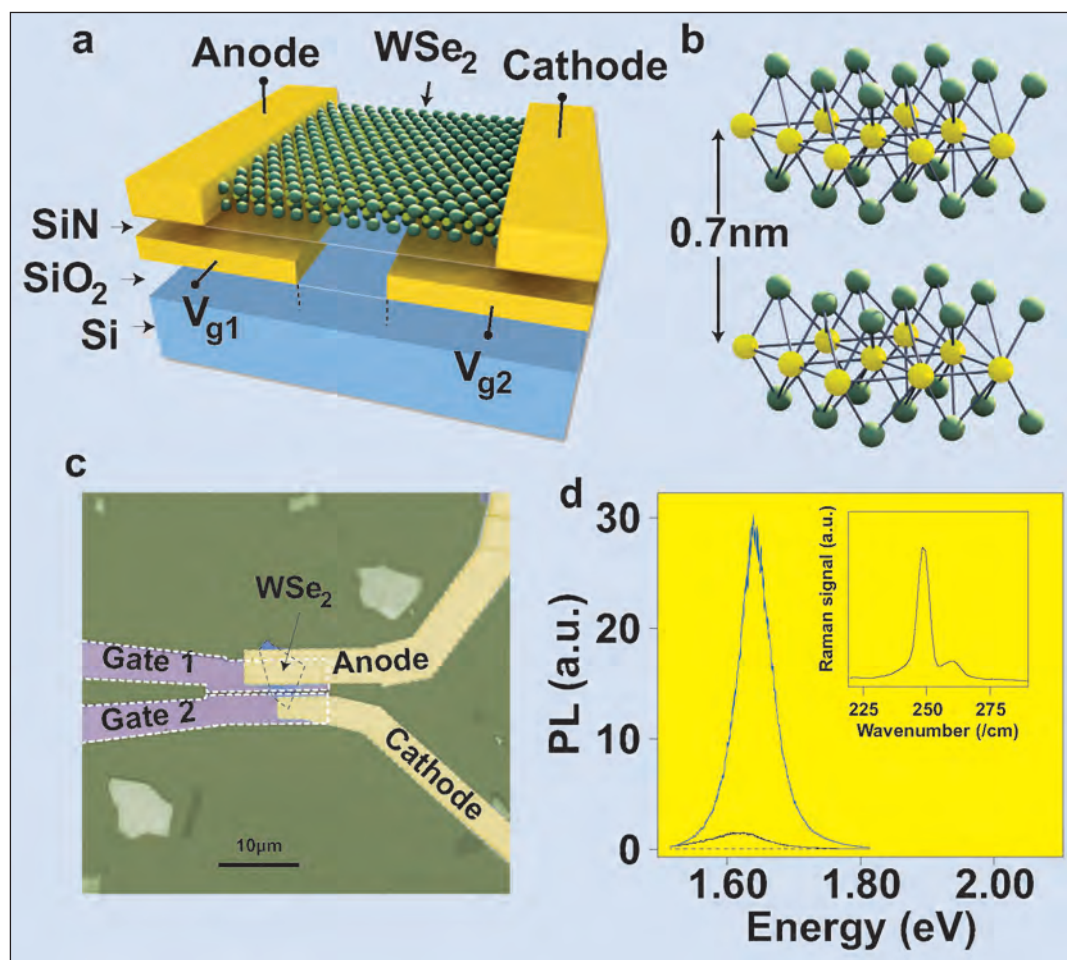


Figure 1. WSe_2 monolayer device with split gate electrodes. **a**, Schematic of device structure. **b**, Three-dimensional schematic representation of WSe_2 . **W**, yellow spheres; **Se**, green spheres. **c**, Colored microscope image of device. **d**, PL from monolayer (solid blue line), bilayer (solid black line) and multilayer (dashed black line) WSe_2 flakes. Inset: Raman spectrum of monolayer.

The monolayer WSe_2 LED had an EL emission peak at 1.547eV , 93meV below that of photoluminescence measurements on monolayer WSe_2 . The researchers "assign the shift to different dielectric environments in both experiments, which influence the exciton binding energy due to Coulomb screening."

The researchers comment on potential applications: "For the future, we envision low-cost, flexible and semi-transparent solar cells that could be deployed on glass facades or other surfaces for energy harvesting. Two-dimensional light-emitting diodes could lead to new generations of large-area lighting units and transparent, flexible displays. We also expect applications in the emerging field of valleytronics."

Valleytronics refers to proposals of controlling valleys of the band structure to achieve new ways to manipulate nature for useful ends.

Massachusetts Institute of Technology [Britton W. H. Baugher et al, *Nature Nanotechnology*, vol 9 (2014), p262] constructed their split gates (20nm gold) with 100nm separation. The high-k gate dielectric consisted of 20nm hafnium dioxide. The structure was

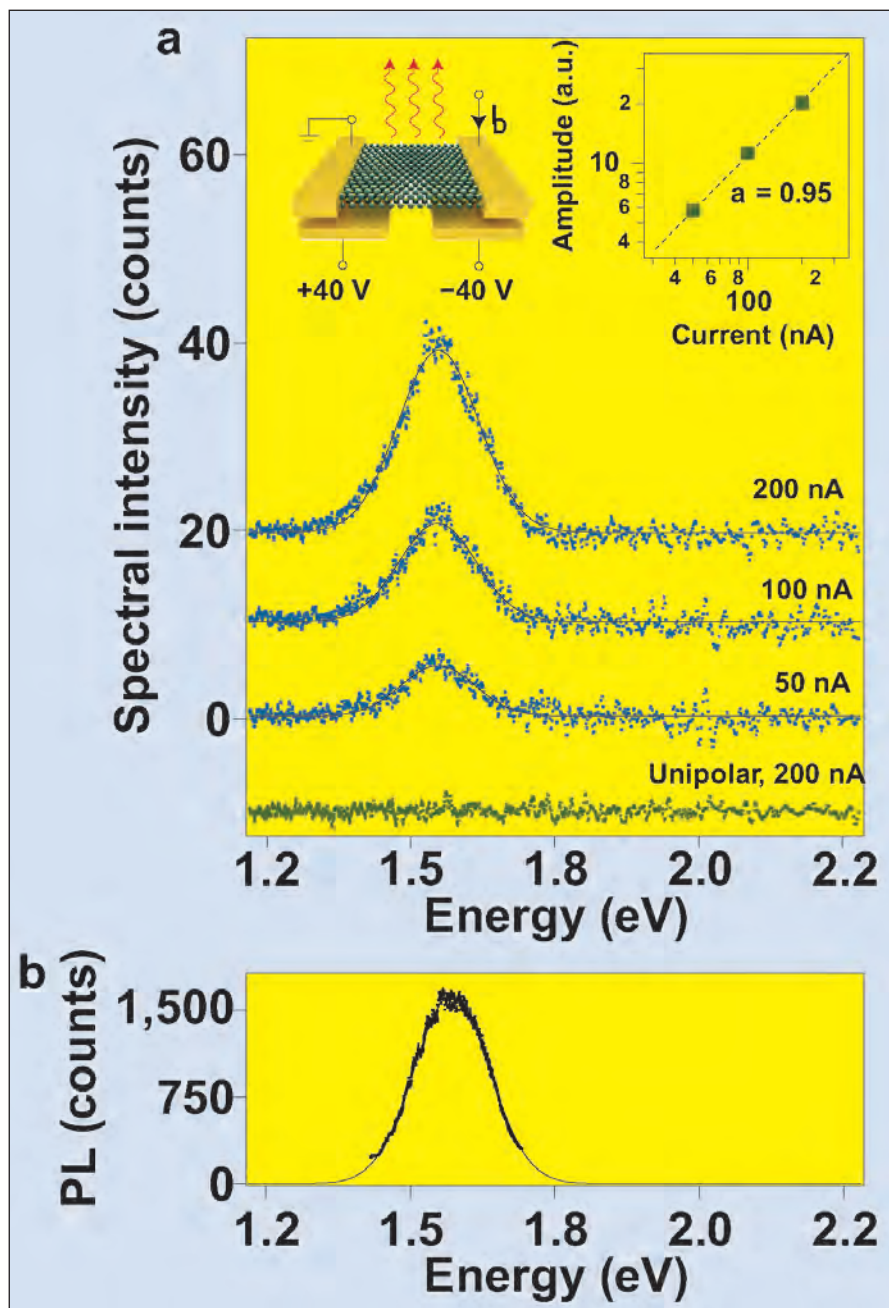


Figure 2. Device operation as LED. **a**, Electroluminescence emission spectra recorded for gate voltages as shown in left inset and constant currents of 50nA, 100nA and 200nA, respectively (blue symbols, measurements; black lines, Gaussian fits). Curves are offset for clarity. Right inset: emission amplitude versus current on a double-logarithmic scale. Symbols, measurements; dashed line, data fit by a power-law I^α , with α close to one ($\alpha \sim 0.95$). **b**, Photoluminescence recorded from WSe_2 flake on device. Symbols, measurements; lines, Gaussian fit.

constructed on highly doped silicon with a 285nm thermal oxide layer. The WSe_2 was transferred to the gate on a stack consisting of glass, polydimethylsiloxane (PDMS) polymer and methyl methacrylate (MMA) resist.

Measurements were made in vacuum at room temperature. The researchers believe that encapsulation methods could be developed to avoid problems with

device degradation from the adsorbates that are present in air.

The MIT researchers also found that the n-type conductivity was higher than the p-type, which they attribute to the lower contact resistance between gold and n-type WSe_2 . The n- and p-type conduction was achieved, respectively, with +10V and -10V gate potentials.

With oppositely biased gates, pn junctions were formed. The current-voltage behavior suggests that recombination dominates over diffusion. "Investigating this recombination, including contributions from Shockley-Read-Hall or Auger processes, will be a focus of future work," the researchers say.

The shunt resistance (leakage) is high at $0.5T\Omega$: "This large shunt resistance indicates a high-quality p-n interface and is an expected advantage of a lateral device geometry." The reverse-bias current was less than 1pA up to 1V. The researchers see this as promising for low-power electronics.

The photoresponse of the device to 532nm wavelengths (green) was as high as 210mA/W, comparable to commercial silicon photodetectors. Spectral measurements from visible to near-infrared wavelengths suggest peaks from the lowest three excitonic levels.

A photovoltaic external quantum efficiency (EQE) peak of 0.2% occurred at 522nm wavelength (Figure 3). The researchers comment: "This value does not take into account the low absorption of monolayer WSe_2 or the narrow cross-section of the p-n junction relative to the size of the laser spot, which together suggest an internal quantum efficiency at least an order of magnitude larger than the EQE reported here."

The researchers attempted to improve the performance for electroluminescence by constructing a device with a palladium p-contact. The light emission peaked at 752nm wavelength (red) with a 2V bias and 100nA injection current. The peak is attributed to a direct-gap exciton transition.

The researchers report: "Using a blackbody source for calibration, we estimate the electroluminescence efficiency, defined as optical output power divided by electrical input power, to be $\sim 1\%$."

The researchers anticipate a "prominent role" for devices based on monolayer dichalcogenide p-n junctions. "Taking into account the three-atom thickness and low optical absorption of monolayer WSe_2 , the responsivity and EQE reported here are quite substantial," the

researchers comment.

They add: "We expect that vertical junctions based on transfer-aligned exfoliated flakes or large-area dichalcogenides grown by chemical vapor deposition could increase responsivity and EQE by more than an order of magnitude. Additionally, improved contact resistance, particularly for holes, should dramatically improve device performance."

A collaboration of researchers from USA, Germany, Japan and China used a ~10nm sheet of smooth, disorder-free hexagonal boron nitride as gate dielectric with 7nm palladium split-gate electrodes. [Jason S. Ross et al, Nature Nanotechnology, vol9, p268, 2014]. The use of boron nitride was designed to "minimize non-radiative energy relaxation pathways".

The structure was supported by a silicon dioxide on silicon substrate. The separation between the gates was 300nm. Gold/vanadium was used for the source/drain contacts, which overlapped the gate regions to reduce the Schottky barrier and provide more ohmic-like carrier injection. The silicon substrate was grounded during measurements.

This research involved University of Washington, USA; Justus Liebig University in Germany, University of Tennessee, USA; Oak Ridge National Laboratory, USA;

National Institute for Materials Science, Japan; and the University of Hong Kong, China.

Again, pn junction behavior was achieved. The maximum photocurrent from a 660nm laser scanned over the sample was 5nA with the gates biased at +8V and -8V. The maximum internal quantum efficiency was estimated at 5%. Photoluminescence studies suggested the presence of neutral excitons (electron-hole bound pairs) and charged trions (bound eeh/ehh), depending on the scan position of the exciting laser spot.

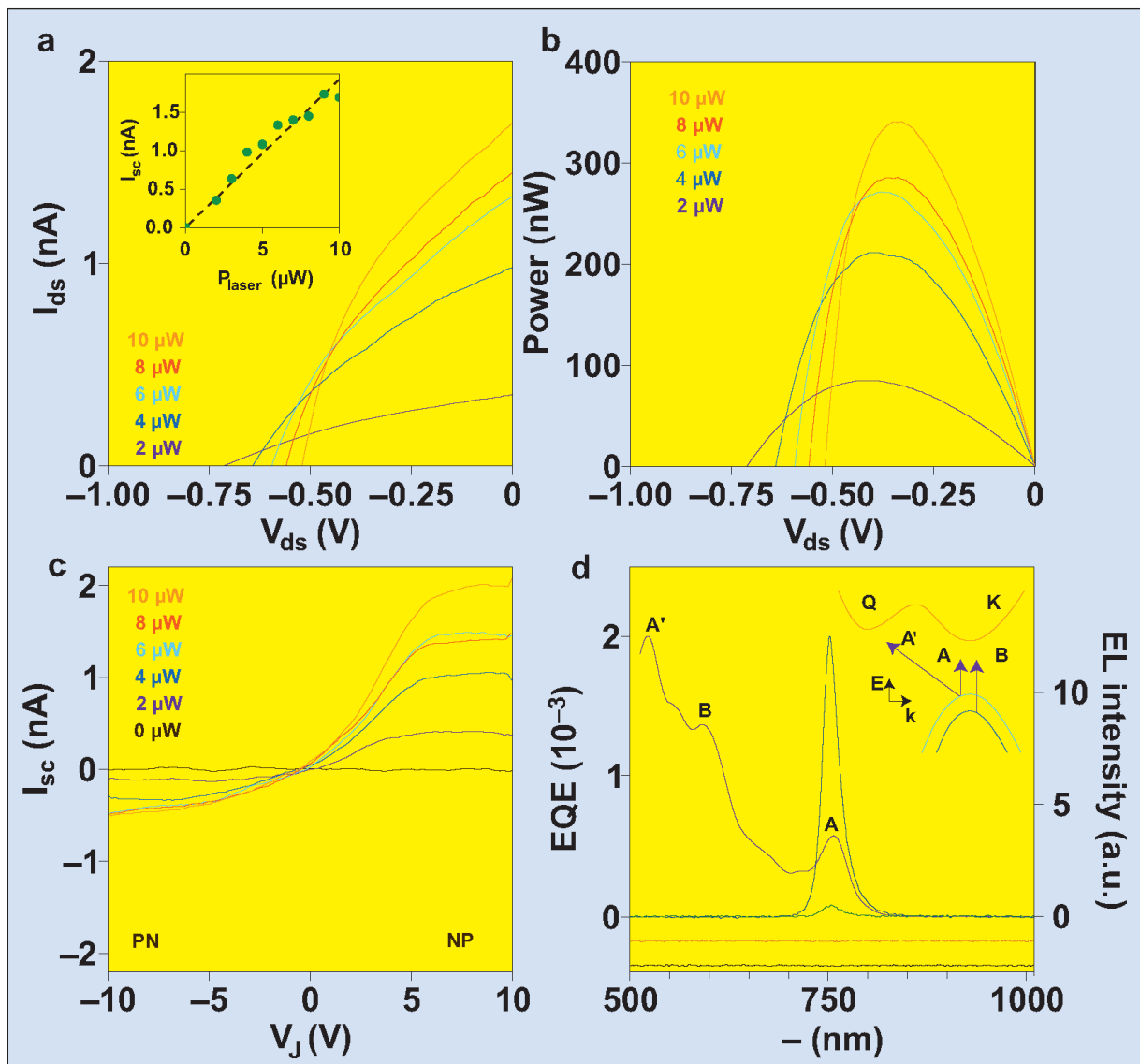


Figure 3. Photovoltaic response and light emission. a, I_{ds} as function of V_{ds} in NP configuration for laser powers 2–10mW (wavelength 700nm). Positive I_{ds} and negative V_{ds} in this regime reflects PV power generation. Inset: short-circuit current I_{sc} (green dots) versus laser power with a linear fit (black dashed line). b, Power $P = I_{ds}V_{ds}$ produced by device as function of V_{ds} for different incident laser powers, calculated from data in a. c, I_{sc} as a function of asymmetric gate voltage, V_J , for different laser powers. d, Left axis: EQE as a function of wavelength at constant laser power of 2mW in NP configuration (purple line). Peaks in EQE correspond to exciton transitions A, B and A', as labelled. Right axis: EL intensity from second monolayer WSe₂ device with one gold and one palladium contact. $V_{ds} = 2V$ in PN (blue trace), NN (yellow trace) and PP (black trace) configurations, and $V_{ds} = -2V$ in NP (green trace) configuration. NN and PP traces are offset vertically for clarity. Inset: Band structure around K and Q points; arrows indicating lowest-energy exciton transitions for monolayer WSe₂.

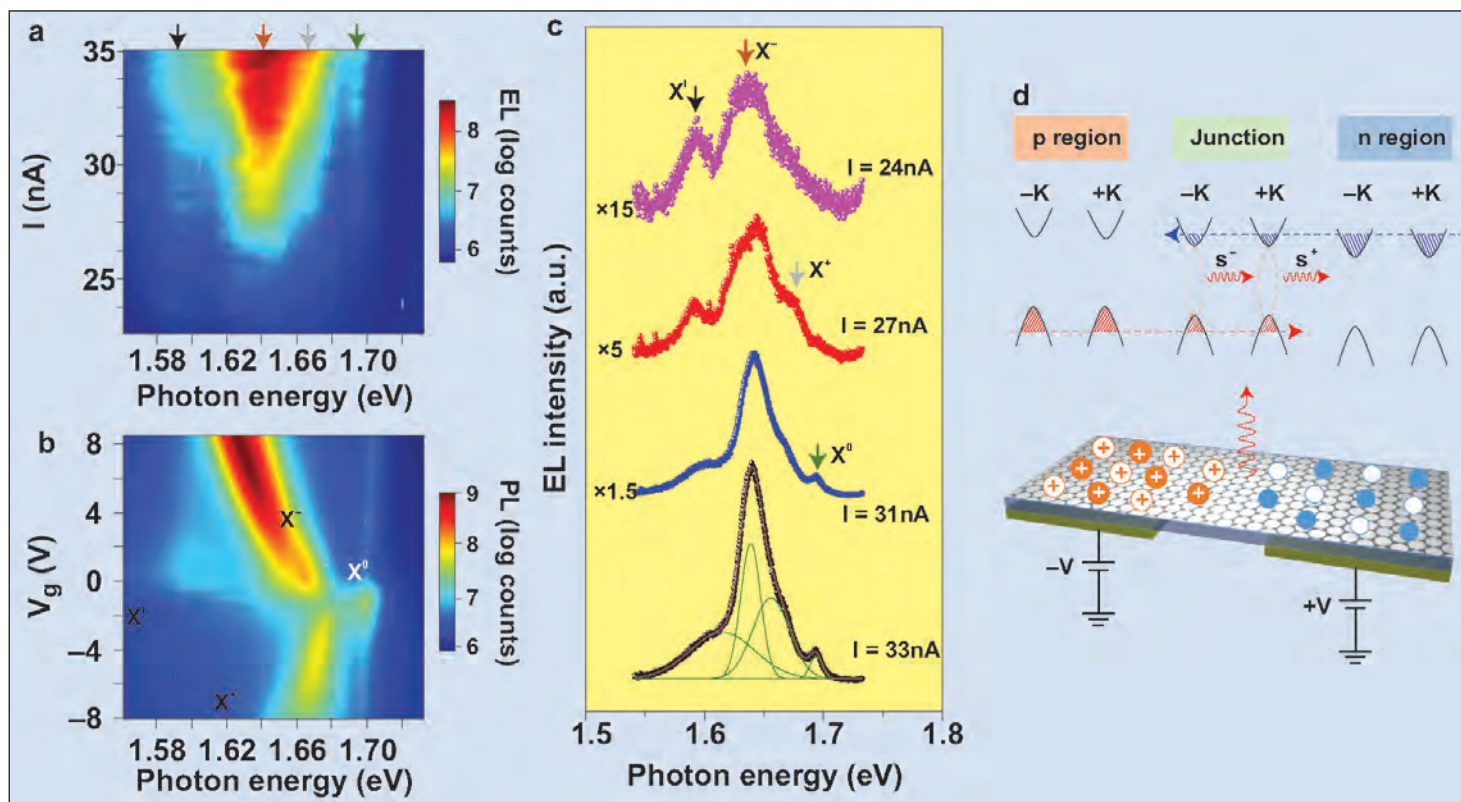


Figure 4. Tuning valley-exciton EL at 60K. **a**, EL intensity plot as function of bias current and photon energy. Left to right, arrows show impurity-bound exciton (X^I), charged excitons (X^- then X^+) and neutral exciton (X^0). **b**, PL intensity as function of photon energy and gate voltage $V_g = V_{g1} = V_{g2}$. **c**, Selected EL spectra at various bias currents. Bottom spectrum is fit by four Gaussian lineshapes, one for each exciton species. **d**, Band diagram and device schematic showing EL generation from valley excitons. Wavy red arrows indicate EL. Dashed red (blue) arrow indicates direction of hole (electron) flow. Filled and empty circles show carriers in $+K$ and $-K$ valleys. Both valleys are shown to be populated, leading to EL with both right (σ^+) and left (σ^-) circular polarization.

► Room-temperature (300K) electroluminescence was observed with currents as low as 200pA. The spectral peak is associated with emission from excitons, “a natural consequence of the large exciton binding energy due to the strong Coulomb interaction in monolayer TMDs,” according to the research team.

A more complex spectral structure was seen in electroluminescence at low temperatures of 60K with contributions from free and bound excitons (X^0 , X^I), and trions (X^- , X^+), with the balance depending on gate voltage and injection current (Figure 4). The trion states were sensitive to changes in the perpendicular electric field across the junction.

The X^0 peak centered on 1.69eV was narrow. The X^- states emitted over a broad range from 1.633–1.625eV, giving the strongest contribution to the spectra. Light from the X^+ trions gave a shoulder to the spectrum around 1.670eV. The bound exciton (X^I) emissions were around 1.59eV. The X^0 linewidth was $\sim 5\text{ meV}$, an order of magnitude smaller than for MoS_2 .

The total photon emission rate at 35nA was 16million/second. The researchers comment: “This is 10 times larger, for 1000 times smaller current, than reported for MoS_2 devices. It corresponds to one photon per 10^4 injected electron–hole pairs.”

It is hoped that better performance could be achieved by reducing the contact resistance, enhancing the WSe_2 crystal quality, and improving the membrane transfer technique. The researchers also believe that ferromagnetic contacts could create spin-polarized injection that would allow the creation of spin- and valley-LEDs with the emission of controllably polarized photons.

The team concludes: “This system has the required ingredients for new types of optoelectronic device, such as spin- and valley-polarized light-emitting diodes, on-chip lasers and two-dimensional electro-optic modulators.”

Finally, researchers in USA and Japan have been seeking better contacts for TMDs by creating nanowires or nanoribbons of the material with a guided electron beam [Junhao Lin et al, *Nature Nanotechnology*, published online 28 April 2014]. It was found that such nanowires/ribbons become more metallic/ohmic for narrow geometries. The collaboration involved Vanderbilt University (USA), Oak Ridge National Laboratory (USA), National Institute of Advanced Industrial Science and Technology (AIST, Japan), University of Tsukuba (Japan), Fisk University (USA) and University of Tennessee (USA). ■

<http://dx.doi.org/10.1038/nnano.2014.14>

<http://dx.doi.org/10.1038/nnano.2014.26>

<http://dx.doi.org/10.1038/nnano.2014.25>